Eur. J. Biochem. **261**, 155–162 (1999) © FEBS 1999

Interaction of purified human proteinase 3 (PR3) with reconstituted lipid bilayers

Wolfgang H. Goldmann[1], John L. Niles[1,2] and M. Amin Arnaout[1]

[1]*Leukocyte Biology and Inflammation Program, Renal Unit and* [2]*Immunopathology, Department of Medicine, Massachusetts General Hospital, Harvard Medical School, Charlestown MA, USA*

Proteinase 3 (PR3), the major target autoantigen in Wegener's granulomatosis is a serine proteinase that is normally stored intracellularly in the primary granules of quiescent neutrophils and monocytes. Upon cell activation, a significant portion of this antigen is detected on the cell surface membrane. The nature of the association of PR3 with the membrane and its functional significance are unknown. We investigated the interaction of purified human PR3 with mixtures of zwitterionic (dimyristoyl-L-α-phosphatidylcholine, DMPC) and anionic (dimyristoyl-L-α-phosphatidylglycerol, DMPG) phospholipids in reconstituted lipid bilayers using differential scanning calorimetry and lipid photolabeling, and measured the affinity of this interaction using spectrophotometry. Two other primary granule constituents, human neutrophil elastase (HNE) and myeloperoxidase (MPO) were investigated for comparison. In calorimetric assays, using lipid vesicles of mixed DMPC/DMPG, increasing PR3 concentrations (protein/lipid molar ratio from 0 to 1 : 110) induced a significant decrease of the main chain transition enthalpy and a shift in chain melting temperatures which is indicative of partial insertion of PR3 into the hydrophobic region of the lipid membranes. This was confirmed by hydrophobic photolabeling using liposomes containing trace amounts of the photoactivable [^{125}I]-labeled phosphatidylcholine analog TID-PC/16. The molar affinity of PR3, HNE, and MPO to lipid vesicles of different DMPC/DMPG ratios was then determined by spectrophotometry. At a DMPC/DMPG ratio of 1 : 1, molar affinities of PR3, K_d = 4.5 ± 0.3 μM; HNE, 14.5 ± 1.2 μM; and MPO, 50 ± 5 μM (n = 3) were estimated. The lipid-associated PR3 exhibited two-fold lower V_{max} and K_m values, and its enzyme activity was slightly more inhibited (K_i) by the natural α_1-proteinase inhibitor (α_1-PI) or an autoantibody to PR3.

Keywords: calorimetry; hydrophobic photolabeling; light scattering; proteinase 3–lipid interaction; Wegener's granulomatosis.

Wegener's granulomatosis (WG) is a systemic vasculitis of unknown etiology that is defined histologically by the presence of necrotizing vasculitis, granulomas, often associated with pauci-immune glomerulonephritis [1]. This disease rarely improves spontaneously and treatment with immunosuppressive drugs such as corticosteroids and cyclophosphamide is essential for the prevention of multiorgan failure. Understanding the mechanism that triggers and perpetuates WG has therefore been the prime aim of much research [2–6].

Proteinase 3 (PR3) is a serine proteinase with potent pro-inflammatory potential that is expressed by phagocytic cells (polymorphonuclear cells, monocytes) of the immune system. PR3 is stored intracellularly in an inactive form in the azurophilic (primary) granules of resting leukocytes [7]. When these cells are activated to ingest microbes, the primary granules fuse with phagosomes. PR3 as well as other hydrolytic enzymes contribute to the eventual digestion of the ingested pathogens. PR3 has, in fact, been directly shown to kill microbes *in vitro*. The antimicrobial activity of PR3 can also proceed without a requirement of its catalytic activity, perhaps through direct insertion into the microbial lipid membrane [8]. Some of the primary granule content is spilled into the extracellular environment during phagocytosis. PR3 and other hydrolytic enzymes released in this way are rapidly inactivated by natural proteinase inhibitors such as α_1-proteinase inhibitor (α_1-PI) which exist in high concentrations in peripheral blood. Significant amounts of PR3 are also found associated with the cell surface membrane of activated leukocytes [7]. The functional significance of this form is unclear, and the mechanism(s) through which PR3 associates with the lipid bilayer is unknown.

In WG, a majority of patients have circulating autoantibodies to different epitopes of PR3 and myeloperoxidase (MPO) [9]. The prevalence of anti-PR3 autoantibodies (so-called anti-neutrophil cytoplasmic antibodies; ANCA) has allowed the development of an ELISA that is currently used as a diagnostic test for WG [4]. The process leading to the initiation of an autoimmune response to PR3 or MPO in WG is unclear. It is presumed that exposure of this otherwise 'hidden' antigen on the cell surface of activated leukocytes may contribute to this process.

In this study, we investigated the nature of the association of PR3, human neutrophil elastase (HNE), and MPO with lipid vesicles. By using a combination of calorimetric,

Correspondence to W. H. Goldmann, Renal Unit, Massachusetts General Hospital, Building 149, Harvard Medical School, Charlestown, MA 02129, USA. Fax: + 1 617 726 5669, Tel.: + 1 617 726 5663.
E-mail: goldmann_w@hub.tch.harvard.edu.

Abbreviations: α_1-PI, α_1-proteinase inhibitor; PR3, proteinase 3; ANCA, antineutrophil cytoplasmic antibody; WG, Wegener's granulomatosis; DMPG, dimyristoyl-L-α-phosphatidylglycerol; DMPC, dimyristoyl-L-α-phosphatidylcholine; HNE, human neutrophil elastase; MPO, myeloperoxidase; Boc-Ala-Onp, N-t-Boc-L-alanine-*p*-nitrophenyl-ester; FITC, fluoresceine isothiocyanate; [^{125}I]TID-PC, ^{125}I-labeled phosphatidyl-choline analog; DSC, differential scanning calorimetry; ES, enzyme–substrate.

(Received 3 November 1998, revised 18 January 1999, accepted 22 January 1999)

spectrophotometric, and lipid photolabeling techniques, we present evidence that PR3 interacts hydrophobically with zwitterionic and anionic phospholipid bilayers and that its enzyme activity is still functional although slightly more sensitive to inhibition by physiologic (α_1-PI) and pathologic (PR3-ANCA) inhibitors.

MATERIALS AND METHODS

Reagents

N-t-Boc-L-alanine-*p*-nitrophenyl-ester (Boc-Ala-Onp) was purchased from Sigma-Aldrich (St Louis, MO, USA) and dissolved in dimethylformamide to 300 mM stock solution. Fluoresceine isothiocyanate (FITC)-elastin (200–400 mesh) was obtained from ICN Biochemicals (Cleveland, OH, USA) and suspended in 50 mM sodium phosphate buffer, pH 5.5 to a final concentration of 1.67 mg·mL^{-1} [10]. α_1-PI was purchased from Sigma.

Proteins

Human neutrophil PR3 was purified by affinity chromatography using monoclonal antibody 1E8 coupled to Sepharose-4B as described previously [3]. HNE and MPO were purchased from Elastin Products Company Inc. (Owensville MO, USA). The purity of PR3, HNE, and MPO was checked routinely by SDS/PAGE [11].

Isolation of IgG

The IgG fraction containing either anti-PR3 or anti-MPO autoantibodies was isolated from the serum of a patient with WG or microscopic polyangiitis, respectively, by ammonium sulfate fractionation, and affinity purified on protein-G agarose columns [10]. Purified IgG from this serum was subsequently referred to as PR3-ANCA.

Lipid vesicles

The phospholipids, dimyristoyl-L-α-phosphatidylcholine (DMPC) and dimyristoyl-L-α-phosphatidylglycerol (DMPG) were purchased from Sigma and used without further purification. Prior to experimentation, a lipid stock solution was prepared by dissolving mixtures (1 mg·mL^{-1}; w/w) of the lyophilized phospholipids in chloroform/methanol, 2 : 1 (v/v). The solvents were quickly evaporated under a stream of nitrogen and a thin lipid film formed on the walls of the glass beaker. This was followed by vacuum desiccation for at least 2 h. Thereafter, the lipids were swollen in 30 mM NaCl, 20 mM Hepes/NaOH, 1 mM dithiothreitol, 2 mM EGTA, pH 7.4 overnight at 42 °C to form vesicles [12].

Differential scanning calorimetry (DSC)

The microcalorimeter has previously been described by Tempel *et al*. [13]. Prior to measurements, the samples were equilibrated at 4 °C for 30 min. Reconstitution of proteins into lipid vesicles was achieved by repeated heating/cooling cycles between 4 °C and 40 °C. The heating/cooling cycles were carried out at a scan rate of 30 °C·h^{-1} and with a filter constant of 15. This method allowed direct observation of the influence of PR3, HNE, and MPO on the lipid phase transition. The measurements with pure lipids were compared with samples in the presence of proteins. After the second to fourth scan, the heat capacity profiles became identical, indicating that the reconstituted lipid/protein system was at equilibrium. All traces were normalized with respect to the lipid concentration in the measuring cell and corrected by the same base line for direct comparison. Data analysis was carried out, using KaleidaGraph™ 3.0 with a weighted fit.

Integration of the area between the solidus line, T_s (onset of the phase transition) and liquidus line, T_l (completion of the phase transition) of the measured heat profiles allows the calculation of enthalpy changes, ΔH, associated with protein binding.

Hydrophobic photolabeling

Liposomes containing the [^{125}I]-labeled phosphatidyl-choline analog ([^{125}I]TID-PC) were prepared as described by Niggli *et al*. [14]. In brief, the liposome solution in 20 mM Hepes, 0.2 mM EGTA, pH 7.4 consisted of phosphatidylserine and 0.001% (v/v) of [^{125}I]TID-PC. Proteins (PR3, HNE, MPO) were dialyzed against 20 mM Tris/HCl pH 7.4, 0.1 mM EDTA, 15 mM mercaptoethanol followed by centrifugation at 20 000 ***g*** at 4 °C for 20 min prior to use. Photolysis and SDS/PAGE were performed as described previously. The Coomassie blue-stained gels were dried and exposed for 4–8 days to Trimax XM films at −70 °C with intensifier screens; radioactivity was measured in a LKB 1272 Clinigamma counter.

Spectrophotometry

Measurements were carried out in a Perkin Elmer Flourolog 50B Spectrophotometer. A metal cell holder – containing the 0.3 mL measuring glass tube – was controlled thermostatically by an external water bath (± 0.1 °C). During measurements, the temperature was increased linearly between 15 °C and 35 °C at a rate of 1.6 °C·min^{-1} (Fig. 2, inset). Proteins and lipid vesicle solutions were added and gently mixed by hand to prevent the formation of air bubbles. The signal was recorded at 380 nm and a 90° angle to the incident light. This wavelength was chosen in order to avoid interference from phospholipid and protein adsorption at 225 nm and 280 nm, respectively. As light at a 90 degree angle can measure the amount of protein bound (in this case, to lipids) and the protein of reflected light in the light path is measured at 380 nm, unbound protein has little influence on the detected signal. Data were collected on an Apple Macintosh IIci computer (program 3.21) and later transferred to a Macintosh IIfx for data analysis.

Theoretical considerations of spectrophotometric measurements

The principle is based on the ability to polarize particles in an electric field, E, by the incident light and hence to generate reflected light [15,16]. When the intensity, I, is equal to the square of E the following relationship can be applied:

$$\ln (I_s/I_0) = -K \cdot b \cdot c \quad (1)$$

where: I_0 is the intensity of the incident light at the start of the phase transition; I_s is the intensity of the reflected light at the end of phase transition; K is a constant; b is the light path; and c is the concentration of the reactant. The constant, $K = (4\pi \cdot k' \cdot n)/\lambda$, consists of: n, the refractive index of the solution; λ, the wavelength; and k' $(M \cdot \sin \phi)/L$ where M is the molecular mass, ϕ is the reflective angle and L is the Avogadro constant. In our analysis of binding reactions the refractive index is assumed to be constant, and the influence of the buffer is regarded as negligible. Using Eqn (1), the ratio of the signal

amplitude, $\ln(I_s/I_0)$, when plotted against protein concentration shows a linear dependence; it is essential to establish this for a concentration-dependent binding reaction.

Enzymatic reactions

The esterolytic activity of PR3 was tested in the presence of autoantibody or α_1-PI and lipid vesicle (DMPC/DMPG 1 mg·mL^{-1}) solutions at ambient temperature using Boc-Ala-ONp as substrate. Prior to experimentation, PR3 concentration near to the K_d was used and the mixture was exposed to four repeated heating/cooling cycles between 4 °C and 35 °C to ensure lipid insertion. Using PR3 + α_1-PI with liposomes, both proteins were premixed prior to photometric experiments under conditions where α_1-PI was in molar excess over PR3, saturating all binding sites on PR3. This procedure was used to ensure any interference (electrostatic, charge–charge interaction) of α_1-PI with membranes. In brief, the enzymatic reaction was started by adding 0.51 μg of enzyme to the reaction buffer containing between 0.1 and 0.5 mM substrate. Changes in OD_{347nm}were recorded continuously in a Hitachi U-2000 photometer. Readings from control experiments (substrate and buffer in the absence of lipids) were used to determine the baseline activity. Proteolysis of elastin was assayed by adding 1.9 μg of PR3 to 0.3 mL reaction buffer and DMPG/DMPC lipid solution containing 0.5 mg FITC-elastin at the same wavelength and temperature. Kinetic analysis was performed using Lineweaver–Burk and Dixon plots [17].

RESULTS

DSC

The ability of PR3 to associate with lipid bilayers was evaluated by measuring the change of excess specific heat with rising temperature for DMPG/DMPC (50 : 50) vesicles in the presence of increasing concentrations of PR3. As shown in Fig. 1, PR3 caused a shift in the main chain melting of lipids to lower temperature, giving the entire phase transition profile an asymmetric contour. The low-temperature shift indicates a protein–lipid interaction, and is believed to originate from conformationally inhibited lipid molecules adjacent to bound proteins which cannot undergo a phase transition [18]. The decrease in sharpness of the phase transition suggests a disruption of the cooperative behavior of the lipid matrix. At the highest protein/lipid molar ratio of 1 : 110, the difference between the pretransition points in the absence and presence of PR3 (T_s* and T_s, respectively) was 0.9 °C (Fig. 1, trace a versus trace f). The small value of this shift is a sign of a small but significant hydrophobic interaction of PR3 with DMPC/DMPG vesicles. The respective T_s* – T_s values for HNE and MPO of 0.5 °C and 0.3 °C reflect weak or minimal interaction with the liposomes. Comparing the total main chain melting transition between T_s* or T_s (pretransition point) and T_l* or T_l (post-transition point), respectively, in protein-free lipid vesicles (Fig. 1, trace a) with lipid vesicles in the presence of PR3 (molar ratio of 1 : 110; Fig. 1, trace f) shows a shift from 6.9 °C to 8.8 °C (shift of 1.9 °C). The values for HNE and MPO under identical conditions showed a shift of 1.0 °C and no shift, respectively, compared to protein-free vesicles (Table 1). These results are indicative of stronger hydrophobic interactions with lipid vesicles for PR3 and weaker interactions for HNE and MPO.

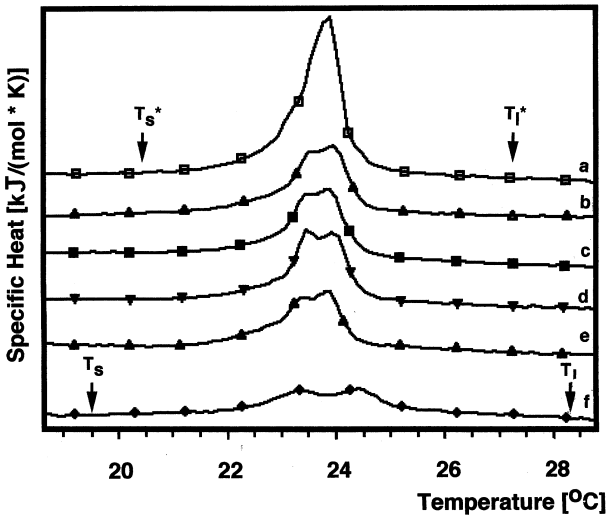

Fig. 1. DSC-measurements of pure and PR3-reconstituted mixed lipid vesicles. DSC heating profiles between 15 °C and 35 °C of pure and PR3-reconstituted DMPC/DMPG unilamellar vesicles. The endotherms show the variation of the main phase transition with increasing concentrations of PR3. The incubation protein/lipid molar ratios of the endotherms were: (a) 0 (pure lipids); (b) 1 : 2050; (c) 1 : 770; (d) 1 : 450; (e) 1 : 325; (f) 1 : 110. The scans are normalized and baseline-corrected. T_s* and T_l* and T_s and T_l indicate the (pre- and post-transition points) for pure lipids (a) and lipids in the presence of PR3 (f), respectively.

Hydrophobic photolabeling

To complement the lipid binding studies using DSC, hydrophobic photolabeling was carried out to compare the degree of association of PR3, HNE and MPO with the hydrophobic region of lipid bilayers. Results from these experiments are shown in Table 2. PR3 incorporates significant amounts of radioactivity when incubated and photolyzed in the presence of liposomes containing trace amounts of photolabel. HNE and MPO also incorporate into the hydrophobic region of lipid membranes but to a much lesser degree. Little to no incorporation of IgG is observed. These data support the findings obtained by DSC that PR3 inserts into the hydrophobic region of negatively charged lipid bilayers. HNE and MPO incorporate to a much lesser extent in comparison.

Table 1. Lipid melting temperatures in the presence of PR3, HNE, and MPO. Lipid melting temperatures at protein/lipid molar ratios of 1 : 110 as determined from baseline-corrected DSC measurements.

	Lipid melting temperature (°C)			
Lipid melting transition points and shift	PR3	HNE	MPO	DMPG/DMPC (control)
Pre-transition point (T_s or T_s*)	19.5	19.9	20.1	20.4
Post-transition point (T_l or T_l*)	28.3	27.8	27.0	27.3
(T_l–T_s) or (T_l*–T_s*)	8.8	7.9	6.9	6.9
Shift [(T_l–T_s) or (T_l*–T_s*)]	1.9	1.0	0	–

Table 2. Hydrophobic photolabeling of PR3, HNE and MPO upon incubation with liposomes containing trace amounts of photoactivatable phospholipids. Proteins were preincubated in the absence of liposomes for 15 min at room temperature. Liposomes containing trace amounts of [I^{125}]TID-PC/16 were then added to the proteins and incubation was continued for a further 15 min. Final concentrations were 1.25 mg·mL^{-1} lipids and 0.16 mg·mL^{-1} proteins (PR3, HNE, MPO). Bovine IgG (control) at 0.1 mg·mL^{-1} was treated in the same way. The samples were then photolyzed and analyzed by autoradiography.

		[^{125}I] Incorporated (c.p.m. per 3.4 μg)			
Experiment	Photolysis	PR3	HNE	MPO	IgG
1	+	155	31	7	6
	–	13	14	6	0
2	+	125	22	25	4
	–	7	9	7	0

Spectrophotometry

To determine the binding affinity of PR3 to liposomes, we used spectrophotometric measurements. The intensity, $I = I_s/I_0$ of various total protein/lipid solutions was detected at a 90° angle to the incident light, at a wavelength of 380 nm and at linear temperature increases between 10 °C and 35 °C. The amplitude, which reflects the gel-to-liquid crystalline main-phase transition at 23.8 °C of DMPC/DMPG (50 : 50; w/w) vesicles, changes at different concentrations of PR3 (Fig. 2): with increasing protein concentration, the averaged traces reveal a gradual decrease in signal amplitude; at a PR3/lipid molar ratio of 1 : 110 (Fig. 2f), the amplitude at 23.8 °C is greatly reduced compared to that of lipids in the absence of protein (Fig. 2a). The reduction in the signal amplitude could be caused by conformational restrictions in phase transition of lipid molecules adjacent to bound protein.

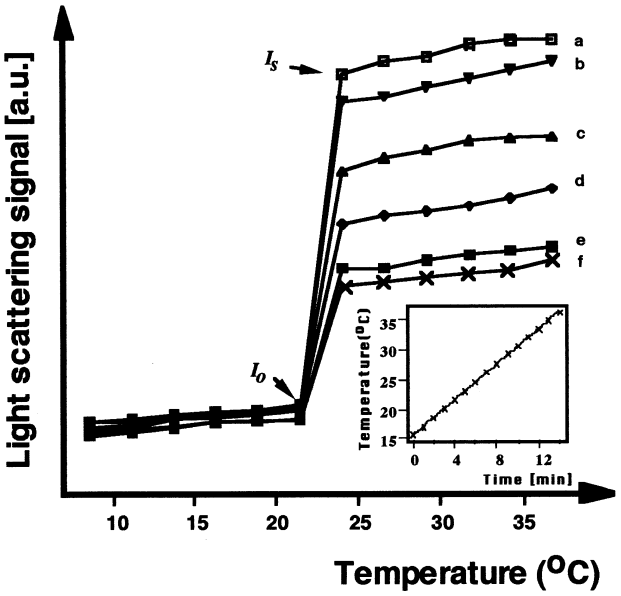

Fig. 2. Spectrophotometric measurements of pure and PR3-reconstituted mixed lipid vesicles. Temperature-induced changes in reflective signal between 15 °C and 35 °C at a rate of 1.6 °C·min^{-1} of a 0.3-mL solution, containing various PR3 concentrations: (a) 0 μM; (b) 1.25 μM; (c) 2.5 μM; (d) 4.5 μM; (e) 13.5 μM; (f) 25.5 μM. I_0 and I_s indicate the start and the end of the signal at 380 nm for the main phase transition of DMPC/DMPG at 23.8 °C. The traces represent averages of four heating scans. The inset shows a linear temperature increase of 1.6 °C·min^{-1}. Using equation (1), the ratio of the signal, $\ln(I_s/I_o)$, when plotted against protein concentration, shows a linear dependence (inset). Experimental conditions were as described in Fig. 1.

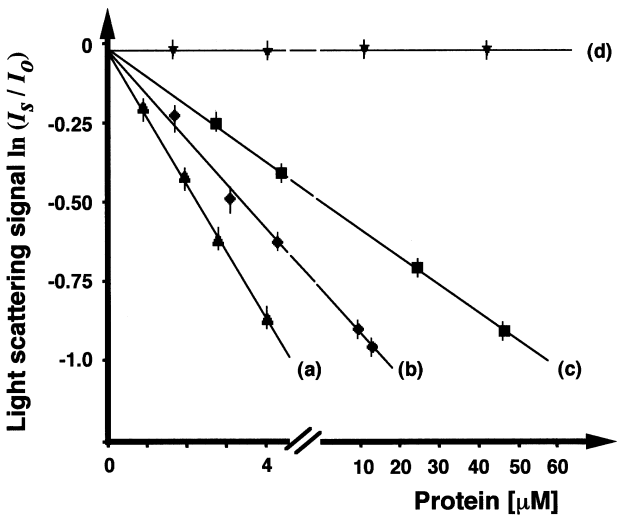

Fig. 3. Plots of observed light signal for PR3, HNE and MPO reconstituted into mixed lipid vesicles. Observed reflective light signal at 23.8 °C and 380 nm plotted against protein concentration for PR3, HNE and MPO. The equation $\ln(I_s/I_0) = -K{\cdot}b{\cdot}c$ was used to calculate the slope, K. K_d values were calculated for PR3 (a), HNE (b) and MPO (c) from the relationship $1/K = K_d$. (d) The reflective signal was measured in control experiments, performed under identical conditions, using various ovalbumin concentrations and 1.46 mM DMPC/DMPG (50 : 50; w/w). The lines represent the best fit to the data; data shown are means of triplicate experiments; SD < 5%.

We next determined the molar affinity of PR3, HNE and MPO for charged phospholipid vesicles. We measured the reflected light signal at 380 nm for solutions before and after the main phase transition (23.8 °C) and plotted the data against various protein concentrations, using the linear equation, $\ln (I_s/I_0) = -K{\cdot}b{\cdot}c$. From the best linear fit to the data, molar affinity (K_d) values of protein to DMPC/DMPG (50 : 50) lipid vesicles were calculated to be 4.5 μM for PR3, 14.5 μM for HNE, and 50 μM for MPO, respectively (Fig. 3). The affinity calculated for PR3 compares well with published data for vinculin (K_d = 3 μM) [19], a protein known to be membrane-associated, whereas the affinities of HNE and MPO for DMPC/DMPG (50 : 50) lipid vesicles are of less significance. A similar analysis using lipid vesicles of different compositions revealed that the protein/lipid affinities were highest for DMPC/DMPG (50 : 50) lipid vesicles (Table 3). This ratio was therefore used throughout all subsequent experiments.

Effect of lipids on PR3 enzymatic activity

To evaluate the effect of lipid membrane association on the enzymatic activity of PR3, the rate of hydrolysis of the PR3 substrate Boc-Ala-ONp [10] by free and membrane-associated PR3 was measured. The hydrolysis reaction reached steady state at ambient temperature within 15 min at concentrations between 0.1 and 0.5 mM of substrate, and results from three separate experiments are shown in Fig. 4. The enzyme activity of PR3 shows a linear dependence on substrate concentration, indicating no allosteric effect in the presence or the absence of liposomes. Lipid-associated PR3 displayed a parallel shift in the slope, reducing the values for V_{max} and K_m by 50% (K_m = 0.25;

Table 3. K_d for the binding of proteins to liposomes containing various ratios of DMPC to DMPG. K_d (μM)for liposomes consisting of various ratios of (zwitterionic) uncharged (DMPC) and (anionic) charged (DMPG) lipids and PR3, HNE and MPO. The highest affinity was measured for liposomes composed of DMPC/DMPG 50 : 50 for all proteins. Talin and vinculin were used as positive controls and carbonic anhydrase was used as a negative control. Standard deviations are as indicated. Data shown are means of triplicate experiments. Experimental conditions were as described in Fig. 1.

	Lipids				
Proteins	DMPC	DMPC/DMPG 70 : 30	DMPC/DMPG 50 : 50	DMPC/DMPG 30 : 70	DMPG
PR3	85	37 ± 3	4.5 ± 0.3	7.5 ± 1	14.5 ± 1.5
HNE	NB	95 ± 9	14.5 ± 1.2	20 ± 2	22 ± 2
MPO	NB	NB	50 ± 5	68 ± 10	80 ± 10
Carbonic anhydrase	NB	NB	NB	NB	NB
Talin	ND	ND	0.4	ND	ND
Vinculin	ND	ND	3.0	ND	ND

NB, no binding; ND, not determined.

V_{max} = 1 in the presence of lipids, and K_m = 0.5; V_{max} = 2 in the absence of lipids). This 'uncompetitive inhibition' pattern reflects a lower reaction velocity caused by a reduction in enzyme–substrate affinity. In only one of a total of four experiments was a 'mixed-type inhibition' observed under the same conditions.

Susceptibility of lipid-associated PR3 to inhibitors

In further experiments, we examined whether the access of the natural or pathologic inhibitors α_1-PI and autoantibody (PR3-ANCA), respectively, is altered when PR3 is lipid-bound. We found that the presence of lipids slightly increased the inhibitory effect of the α_1-PI on PR3 activity (Fig. 5A). This is also reflected by the inhibition constant, K_i of 3.3 μM in the presence and 4.5 μM in the absence of lipids (Fig. 5B and inset). As the association of PR3 with the lipid bilayer (Fig. 5C) indicates that no simultaneous insertion of the inhibitor in the lipid bilayer occurs, the 'noncompetitive' effect observed in Fig. 5B could probably be due to structural changes upon α_1-PI binding to PR3.

The ability of the purified PR3-ANCA to inhibit the elastinolytic and esterolytic activity of PR3 in the presence and absence of lipids was also measured. Fig. 6A shows the dose–response curve of PR3-ANCA on PR3 activity as determined by fluorometric assays. The inhibition of lipid membrane-associated PR3 was around 80% at a PR3/IgG molar ratio

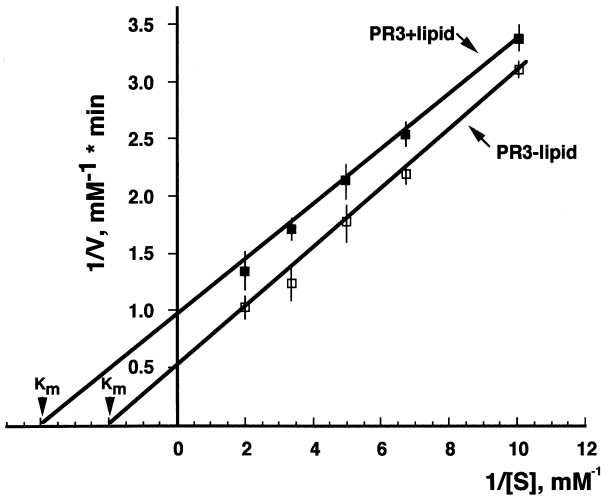

Fig. 4. Enzymatic activity of liposome-incorporated PR3. Plot of PR3 activity in the presence (■) and absence (□) of DMPC/DMPG liposomes using Boc-Ala-ONp as substrate over a concentration range of 0.1–0.5 mM. The kinetic parameters were calculated by linear regression. Data shown are means of triplicate experiments; SD < 7%. Experimental conditions were as described in Fig. 1.

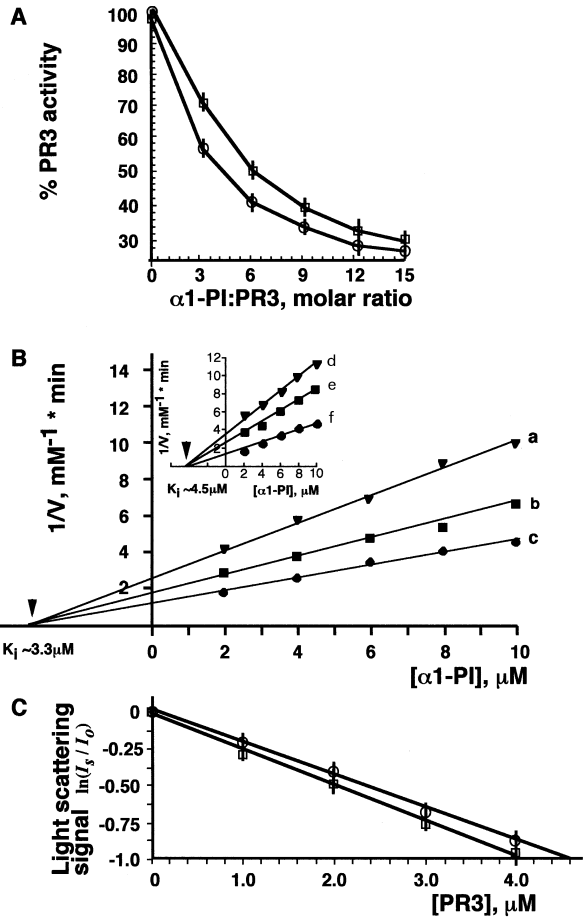

Fig. 5. Insertion of PR3 into lipid membranes and the inhibition of its esterolytic activity by α1-PI. (A) Inhibition of the activity of PR3 bound to α_1-PI. At a PR3/α_1/PI molar ratio of 1 : 15, the esterolytic activity is inhibited by ≈70% □, Without lipids; O, with lipids. (B) Dixon plot analysis to determine K_i in the presence of lipids and (a) 0.1 mM Boc-Ala-ONp, (b) 0.33 mM Boc-Ala-Onp, (c) 0.5 mM Boc-Ala-Onp. Inset: K_i in the absence of lipids and the presence of (d) 0.1 mM Boc-Ala-Onp, (e) 0.33 mM Boc-Ala-ONp, (f) 0.5 mM Boc-Ala-ONp. Data shown are the means of triplicate experiments; SD < 5%. (C) Reflective light signal, $\ln(I_s/I_0)$, of increasing concentrations of PR3 inserted into liposomes in the absence (□) and in the presence (O) of α_1-PI. Experimental conditions as in Fig. 1.

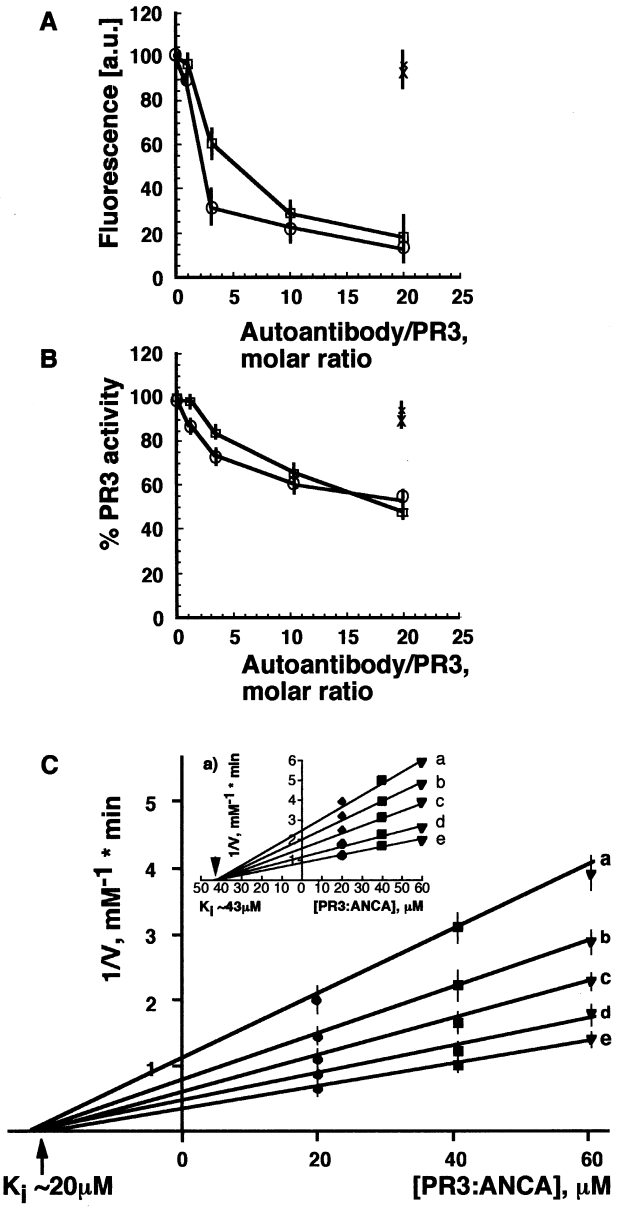

Fig. 6. Inhibition of the esterolytic and elastinolytic activity of PR3 with varying PR3/ANCA concentrations. Inhibition of the elastinolytic (A) and esterolytic (B) activity of PR3 with increasing autoantibody/PR3 molar ratio: □, autoantibody/PR3; ○, autoantibody/PR3 + lipids. Controls: X, autoantibody/MPO; x, autoantibody/MPO + lipids. (C) Inhibition constant, K_I, calculated in the presence and absence (inset) of lipids at various PR3/ANCA and (a) 0.1 mM Boc-Ala-Onp, (b) 0.15 mM Boc-Ala-Onp, (c) 0.2 mM Boc-Ala-Onp, (d) 0.4 mM Boc-Ala-Onp, (e) 0.5 mM Boc-Ala-ONp. Data shown are means of triplicate experiments; SD < 5%. Experimental conditions were as described in Fig. 1

of 1 : 20. At this concentration, inhibition of the elastinolytic activity was unaffected by the presence of lipids. To assess the effect of PR3-ANCA on the esterolytic activity of PR3, PR3-ANCA was preincubated with PR3 in the presence and absence of liposomes, and the enzyme activity measured at various PR3/antibody molar ratios, in the presence of 0.20 mM Boc-Ala-ONp. At a PR3/ANCA molar ratio of 1 : 20 (at which inhibition was maximal), the inhibition observed in the presence and absence of liposomes was 57% and 50%, respectively (Fig. 6B). To evaluate this further, Dixon plot analyses of the membrane-associated PR3 activity in the presence of increasing concentrations of PR3/ANCA and at varying amounts of substrate (0.1–0.5 mM) was carried out. This analysis revealed 'noncompetitive' inhibition with an apparent K_i of ≈20 μM in the presence of lipids (Fig. 6C) compared to a K_i of ≈43 μM in the absence of lipids (Fig. 6C, inset), thus suggesting a somewhat higher degree of inhibition of PR3 when associated with lipids.

DISCUSSION

The major findings in this report are that PR3 partially inserts into artificial lipid membranes, and that this interaction reduces the V_{max} and K_m proportionately, and slightly increases the access of the enzyme to physiologic (α_1-PI) or pathologic (PR3-ANCA) inhibitors.

The incubation of increasing amounts of PR3 with charged liposomes shifts the temperature of onset of chain melting (T_s*→T_s) significantly to lower values, and the temperature of completion of chain melting (T_l*→T_l) to higher temperatures as assessed by DSC (Table 1). This behavior can be explained by two effects: (a) the attachment of PR3 to the membrane surface stabilizes and condenses the bilayer; and (b) the hydrophobic interaction expands and rearranges the lipid bilayer core which leads to a change in transition temperatures. As shown by spectrophotometric measurements, the nature of the interaction depends largely on the lipid composition. Purely uncharged DMPC and charged DMPG vesicles have a lower affinity for PR3 compared to a mixture of charged/uncharged vesicles which have the highest affinity at a molar ratio of 1 : 1 (DMPC/DMPG) (Table 3). This is also observed for the homologous HNE and MPO, although at much lower affinity, which indicates that some membrane surface charge is needed to allow for protein attachment and probably insertion. This phenomenon has been described for various protein–lipid interactions previously [13,20,21]: Niggli *et al.* [14] observed in hydrophobic labeling experiments that both electrostatic and hydrophobic forces are needed for talin and vinculin, two membrane-associated proteins, to insert into lipid bilayers; DeKruijff [22] suggested an initial electrostatic interaction which then facilitates subsequent protein insertion into the membrane.

Having shown that PR3 inserts into the hydrophobic region of liposomes, the viability of this enzyme in the lipid environment and its accessibility to the natural and pathologic inhibitors (α_1-PI and PR3-ANCA respectively) was investigated. The attachment of PR3 to liposomes decreased the esterolytic activity by 50% compared with controls (in the absence of lipids) and displayed an 'uncompetitive inhibition' pattern, whereby the inhibitor (in this case, lipid) reacted reversibly with the enzyme–substrate (ES) complex, thus reducing the enzyme activity [23]. The possibility that the formation of the ES complex induces a conformational change in the tertiary or quaternary structure of PR3 to allow for the inhibitor to interact is not supported by our finding that the presence of substrate has no impact on the association of PR3 with liposomes.

The binding of the natural inhibitor (α_1-PI) to PR3 showed a higher reduction of the enzyme activity in the presence than in the absence of liposomes, documented by the difference in K_i (Fig. 5B and inset), without affecting the level of insertion of PR3 in liposomes (Fig. 6C). The kinetic mechanism is of a 'noncompetitive' nature. The small K_i value for the lipid-bound PR3 suggests that the lipid bilayer influences the 'proper positioning' of PR3 for the substrate and/or impairs the active site. The autoantibody (ANCA) bound to PR3 in the presence of lipids was slightly more effective in noncompetitively inhibiting its activity compared to free PR3 (Fig. 6). These findings

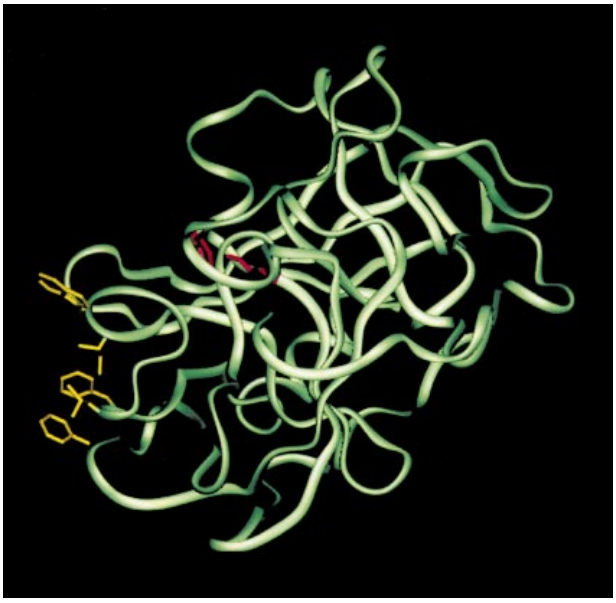

Fig. 7. Hydrophobic region on PR3. A ribbon diagram of human PR3 monomer based on its three-dimensional crystal structure [6]. The hydrophobic patch consists of residues Phe166, Ile217, Trp218, Leu223, Phe224 (yellow) on the surface of PR3. The catalytic site His57, Ser195 and Asp102 are indicated in red. The hydrophobic patch forms one wall of the central cavity of the crystallographic tetramer. The N-terminus lies exposed at the 'bottom' of the enzyme. The figure was constructed using the computer program QUANTA (Biosym/Molecular Simulations, Inc. CA, USA).

suggest that the catalytic and antigenic sites on PR3 are still accessible to the inhibitors when the enzyme inserts into the lipid bilayer.

The three-dimensional crystal structure of PR3 [6] is similar to other serine proteases in the chymotrypsin family. The compact, globular, monomeric protein consists of two β-barrel domains with a large solvent-accessible surface (cf. Fig. 7) which forms a tetramer in crystals. This quarternary arrangement allows for the formation of a hydrophobic 'pore-like' structure, with Phe166, Ile217, Trp218, Leu223 and Phe224 from each monomer contributing to this hydrophobic patch and the formation of the central cavity of the crystallographic tetramer. The catalytic triad (Ser195, His57 and Asp102) and the putative substrate-binding site lie within a shallow depression on the 'front' surface of the protein. A major antigenic loop for ANCA, predicted by Williams *et al*. [9] (residues 108–124) is situated on the 'back' surface of the molecule and is relatively remote from the catalytic and substrate-binding pocket. It is intriguing to speculate, given our results, that the hydrophobic patch may be involved in the insertion of PR3 into the lipid membrane. This may result in the observed small reduction in the accessibility of the substrate (or α_1-PI) to the active site perhaps by a conformational change. Although mapping studies for our PR3-ANCA have not been performed, the major antigenic loop identified for other PR3-ANCA antibodies [6] suggest that at least in this case, the respective epitopes should remain extracellular and accessible to immune modulation. The measured two-fold inhibition of K_m in the presence of lipids (Fig. 6C) probably results from unfavorable orientation of the enzyme–antibody complex on the surface of the membrane.

Our description of the interaction of PR3 with phospholipid membranes suggests a basis for the observed association of this enzyme with the cell membrane of intact cells following activation [24]. Whether additional surface receptor(s) also contribute to this interaction remains to be determined. Current investigations focus on this issue as well as the biological implications for the association of an active proteinase with the leukocyte cell surface and the impact that such an association may have on the pathogenesis of autoimmune vasculitis [25].

ACKNOWLEDGEMENTS

The authors thank D. Scott, C.P. Sharma, and D. Griffith for helpful comments. This work was supported by DK42722 from the National Institutes of Health. Excerpts of this work were presented at the annual ASN Meeting (1997) in San Antonio as a communication and published in abstract form in *J. Am. Soc. Nephrol* **8** (suppl.), 456 A. W. H. Goldmann is a recipient of a collaborative research grant from the North Atlantic Treaty Organization since 1994.

REFERENCES

1. Fauci, A.S., Haynes, B.F., Katz, P. & Wolff, S.M. (1983) Wegener's granulomatosis: prospective clinical and therapeutic experience with 85 patients for 21 years. *Ann. Intern. Med.* **98**, 76–85.
2. van der Woude, F.J., Rasmussen, N., Lobatto, S., Wiik, A., Permin, H., van Es, L.A., van der Giessen, M. & van der Hem, G.K. (1985) Autoantibodies against neutrophils and monocytes: tool for diagnosis and marker of disease activity in Wegener's granulomatosis. *Lancet* **1**, 425–429.
3. Niles, J.L., McCluskey, R.T., Ahmad, M.F. & Arnaout, M.A. (1989) Wegener's granulomatosis autoantigen is a novel serine protease. *Blood* **74**, 1888–1893.
4. Niles, J.L., Pan, G.L., Collins, A.B., Shannon, T., Skates, S., Fienberg, R., Arnaout, M.A. & McCluskey, R.T. (1991) Antigen-specific radioimmunoassays for anti-neutrophil cytoplasmic antibodies in the diagnosis of rapidly progressive glomerulonephritis. *J. Am. Soc. Nephrol.* **2**, 27–36.
5. Rao, N.V., Wehner, N.G., Marshall, B.C., Gray, W.R., Gray, B.H. & Hoidal, J.R. (1991) Characterization of proteinase-3 (PR3), a neutrophil serine proteinase. *J. Biol. Chem.* **266**, 9540–9548.
6. Fujinaga, M., Chernaia, M.M., Halenbeck, R., Koths, K. & James, M.N.G. (1996) The crystal structure of PR3, a neutrophil serine proteinase antigen of Wegener's granulomatosis antibodies. *J. Mol. Biol.* **261**, 267–278.
7. Csernok, E., Ludemann, J., Gross, W.L. & Bainton, D.F. (1990) Ultrastructural localization of proteinase 3, the target antigen of anti-cytoplasmic antibodies circulating in Wegener's granulomatosis. *Am. J. Pathol.* **137**, 1113–1120.
8. Campanelli, D., Detmers, P.A., Nathan, C.F. & Gabay, J.E. (1990) Azurocidin and a homologous serine protease from neutrophils: differential antimicrobial and proteolytic properties. *J. Clin. Invest.* **85**, 904–915.
9. Williams, R.C. Jr, Staud, R., Malone, C.C., Payabyab, J., Byres, L. & Underwood, D. (1994) Epitopes on proteinase-3 recognized by antibodies from patients with Wegener's granulomatosis. *J. Immunol.* **152**, 4722–4737.
10. Daouk, G.H., Palsson, R. & Arnaout, M.A. (1995) Inhibition of proteinase 3 by ANCA and its correlation with disease activity in Wegener's granulomatosis. *Kidney Int.* **47**, 1528–1536.
11. Laemmli, U.K. (1970) Cleavage of structural proteins during the assembly of the head of bacteriophage T4. *Nature* **227**, 680–685.
12. Kaufmann, S., Kaes, J., Goldmann, W.H., Sackmann, E. & Isenberg, G. (1992) Talin anchors and nucleates actin filaments at lipid membranes: a direct demonstration. *FEBS Lett.* **314**, 203–205.
13. Tempel, M., Goldmann, W.H., Dietrich, C., Niggli, V., Weber, T., Sackmann, E. & Isenberg, G. (1994) Insertion of filamin into lipid membranes examined by calorimetric, film balance and lipid labeling method. *Biochemistry* **33**, 12565–12572.
14. Niggli, V., Kaufmann, S., Goldmann, W.H., Weber, T. & Isenberg, G.

(1994) Identification of functional domains in the cytoskeletal protein talin. *Eur. J. Biochem.* **224**, 951–957.
15. Hoppe, W. (1982) *Biophysics.* Springer-Verlag, New York.
16. Chu, B. (1974) *Laser Light Scattering.* Academic Press, New York.
17. Segel, I.H. (1968) *Biochemical Calculations.* John Wiley & Son, New York.
18. Lentz, B.R., Carpenter, T.J. & Alford, D.R. (1987) Spontaneous fusion of phosphatidylcholine small unilamellar vesicles in the fluid phase, *Biochemistry* **26**, 5389–5397.
19. Goldmann, W.H., Senger, R., Kaufmann, S. & Isenberg, G. (1995) Determination of the affinity of talin and vinculin to charged lipid vesicles: a light scatter study. *FEBS Lett.* **368**, 516–518.
20. Heise, H., Bayerl, T., Isenberg, G. & Sackmann, E. (1991) Human platelet P-235, a talin-like actin binding protein, binds selectively to mixed lipid bilayers. *Biochem. Biophys. Acta* **1061**, 121–131.
21. Goldmann, W.H., Niggli, V., Kaufmann, S. & Isenberg, G. (1992) Probing actin and liposome interaction of talin and talin–vinculin complexes: a kinetic, thermodynamic and lipid labeling study. *Biochemistry* **31**, 7665–7671.
22. DeKruijff, B. (1994) Anionic phospholipids and protein translocation. *FEBS Lett.* **346**, 78–82.
23. Gutfreund, H. (1995) *Kinetics for the Life Sciences. Receptors, Transmitters and Catalysts*. Cambridge University Press, New York.
24. Jenne, D.E. (1994) Structure of the azurocidin, proteinase 3, and neutrophil elastase genes. Implications for inflammation and vasculitis. *Am. J. Respir. Crit.Care Med.* **150**, S147–S154.
25. Goldmann, W.H., Niles, J.L. & Arnaout, M.A. (1998) Direct binding of purified proteinase 3 to T lymphocytes. *J. Am. Soc. Nephrol.* **9** (suppl.), 55A.